Icarus – the high efficient Cargo Drone

1. Concept advantages

- No hover propeller before the main wing -> better predictability, lower transition speed, less drag during transition and horizontal flight, safe area before main wing for crew
- Aircraft configuration is commonly used for sailplanes-> well known, less risky, highly efficient
- Hover control concept allows to integrate 4 of the six propellers inside the airframe -> less drag
- Extra yaw propellers improve side wind robustness of aircraft during hover
- Mounting of hover propellers near surfaces, where the disturbance forces are created (stabilizer, vertical tail) reduces structural loads
- Pusher propeller instead of puller propeller creates space for front camera, reduces drag (boundary layer ingesting), creates safe are in front of the main wing (no spinning devices)
- Mounting of main drive engine in front part of the fuselage helps to achieve the design c.o.g. position

2. Design Inspirations

After the first basic calculations and concept ideas it was clear, that the aerodynamic efficiency will be the critical aspect of the aircraft design. Because the electrical power system is fully electrical and energy density in electric batteries is still not the best, low energy consumption has highest priority. Sailplanes are the aircrafts with the highest efficiency so far, so a sailplane-like geometry was used as a starting point.

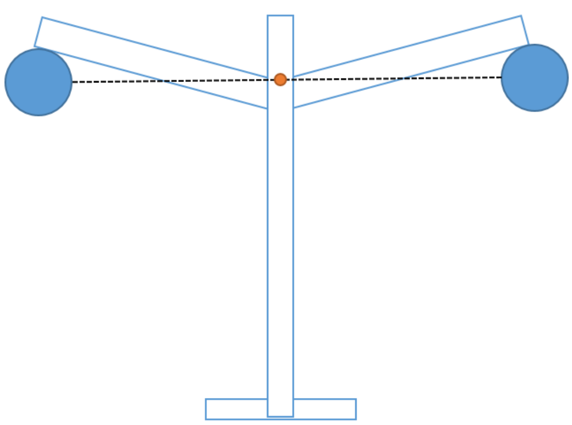

In order to have the main wing flow as undisturbed as possible and because interference effects between hover propeller and the fixed wing are not known so far, the hover propellers are mounted behind the main wing, which leads to a better predictability of the flight mechanics of the airplane and lower drag during transition and therefor lower transition speed. The way to achieve a stable configuration around the y-axis is to sweep the main wing forward and mount the main lift propellers directly behind the main wing. Due to the swept main wing the connection line between the main lifting propellers is still on the main wings center point. Without any perturbations like wind the drone will hover without pitching.

When flying in real conditions, each aerodynamic surface will generate disturbance forces during hover flight. To compensate them, propellers are mounted at each of these surfaces to directly generate the counter force at the point where they appear. Due to the concept with only two main lift propellers, the other propellers can be smaller and integrated near the horizontal stabilizer and the rudder without increasing the drag too much. Moreover, two separate propellers are used to control the yaw axes of the aircraft, which has been done to improve the side wind robustness of the aircraft during hovering. Without these propellers it would only be possible to create a direct yaw moment by using the drag moment of the other main lift propellers.

The drive propeller shall be mounted on the rear end of the drone to exploit two effects. First no rotating parts are before the front wing, which creates a safe area to access the aircraft from the front and second the losses caused by the boundary layer at the rear fuselage is decreased by suction, which is known under the name boundary layer ingesting.

3. Airfoil selection

First an airfoil was selected. For that, the Reynolods number at the design speed is needed. With a mean aerodynamic chord of 250mm the Reynolds number can be calculated to approximately 1*10^6. The Wortmann airfoils work in this Re number well and the following figure suggests to choose an airfoil from the Wortmann catalogue if 500,000<Re<3,000,000.

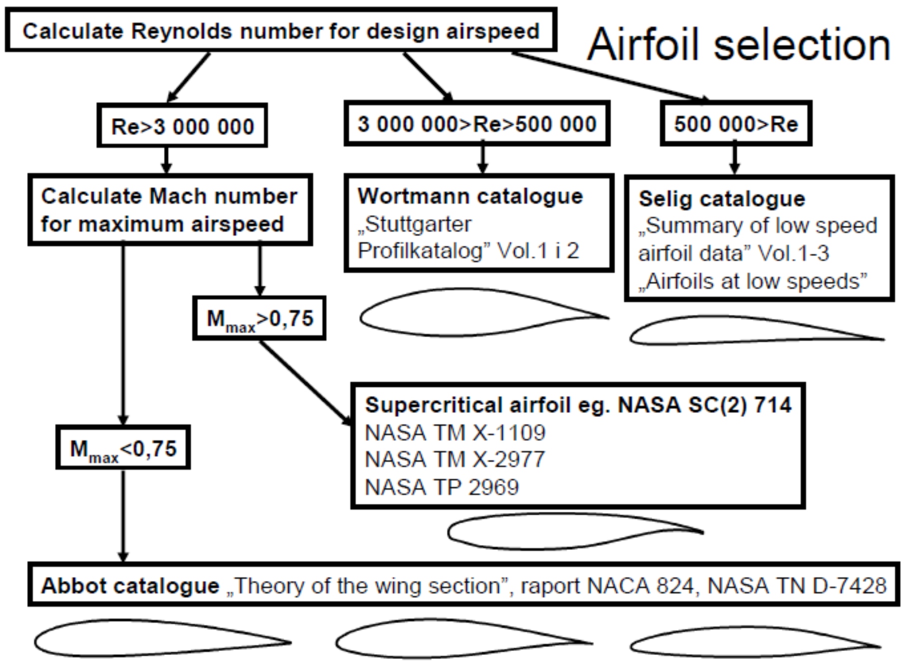

The airfoil selection process is always a compromise between minimum drag at design speed, minimum stall speed and achievable wing stiffness. A good candidate for this design dilemma is the FX 61-163. The following figure shows the profile's geometry:

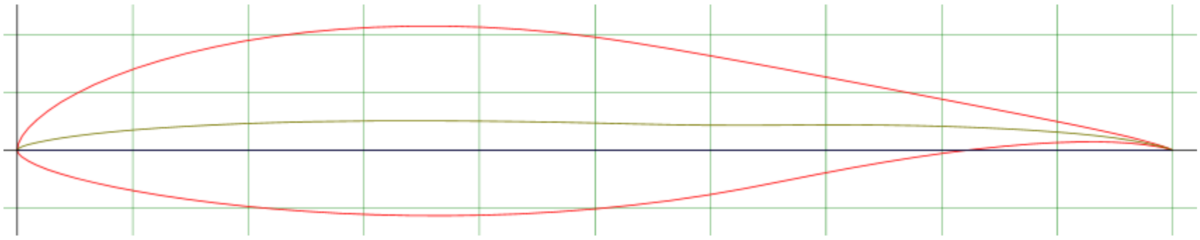

As it can be seen in the figure above, the airfoil has a relatively high maximum thickness, which leads to good attitudes in structural behavior. Nevertheless, it has low drag values and a medium maximum lift coefficient. These facts lead to the choice of this airfoil for the main wing. The following figure shows the lift and drag coefficient of the FX 61-163 airfoil.

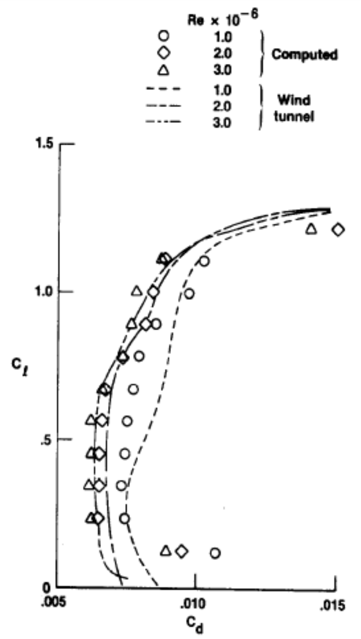

Figure 10. A comparison of computed and wind tunnel data (ref. 3) for the baseline airfoil.

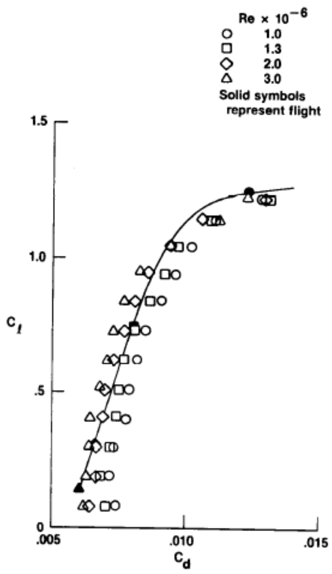

Figure 12. A comparison of computed and flight data (ref. 4) for the flight airfoil with 6° flap deflection.

The used airfoils for the horizontal stabilizer and the vertical tail have to be symmetric and thus the NACA0010 for the horizontal stabilizer and the NACA0010 for the vertical tail have been chosen.

4. Selection of main wing geometry and wing loading

Due to the fact that the propulsion system is purely electrical, the aerodynamic efficiency has highest priority in the design process. The airplanes with the highest aerodynamic efficiency are sailplanes and hence their wing geometry will be used as a starting point. Maximum allowed wing span is 5m and maximum single part length is 2m. Due to the fact that the main wing will consist of two parts (left and right wing) the maximum wing span is approximately 4m plus the fuselage width. The mean aerodynamic chord has been set 0,25m in order to get a good compromise between structural stiffness of the wing and aerodynamic efficiency. Going back to the airfoil data in the figure above, one can see that the highest aerodynamic efficiency is at about CL=0,7. Chosen this lift coefficient as the design lift coefficient would result in the minimum possible CD value at the design speed of 54m/s. However, due to the configuration only about 30% of the total drag are created by the wing itself. The rest is parasite drag from the hover propeller, fuselage, etc., and this parasite drag is independent of the wing loading. The following figure shows the drag over the airspeed for this aircraft concept with two different wing loadings.

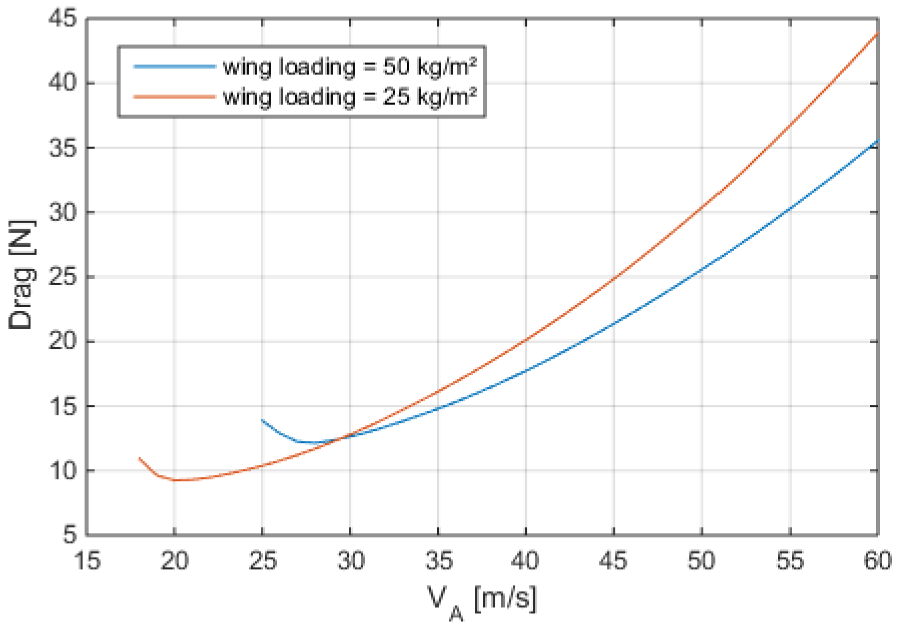

As it can be seen in the figure above, the higher wing loading has a far higher stall speed and only at higher airspeeds the drag is about 20% lower than the version with lower wing loading (25kg/m²). Due to the fact that getting through the transition is critical and as the overall concept will be still able to perform the two missions with a maximum speed of 54m/s the lower stall speed has prioritized over the 20% drag rise at higher speeds. Thus the wing loading has been set to about 25kg/m², which corresponds to a design CL of 0,15. As a consequence the wing area should be about 1m². With the already chosen mean aerodynamic chord of 0,25m and a wing span of 4m, the desired wing area can be achieved. Moreover, a small positive dihedral angle is chosen to get a slightly negative $C_{l\beta}$ value.

The sweep of the main wing and the position of the main lifting propellers has been adjusted iteratively in a way that the c.g. position is directly on the line between the two middle points of the main hover propellers axes, while the main wing is trimmed at the design speed of 54m/s (aerodynamic pitch moment is zero). If the main wing is trimmed at the design speed without the horizontal stabilizer leads to the fact that no lift (positive or negative) is produced at the horizontal stabilizer, which is intended due to the fact that the horizontal stabilizer has a small aspect ratio and thus would create a lot of induced drag by producing lift. In general, the tilting of all other components (fuselage etc.) has been adjusted in a way that they produce minimum drag at the design speed of 54m/s in order to still be able to perform the two required missions.

5. Selection of disc loading for the main lifting propellers

The following figure shows the required hover power over the hover propeller area.

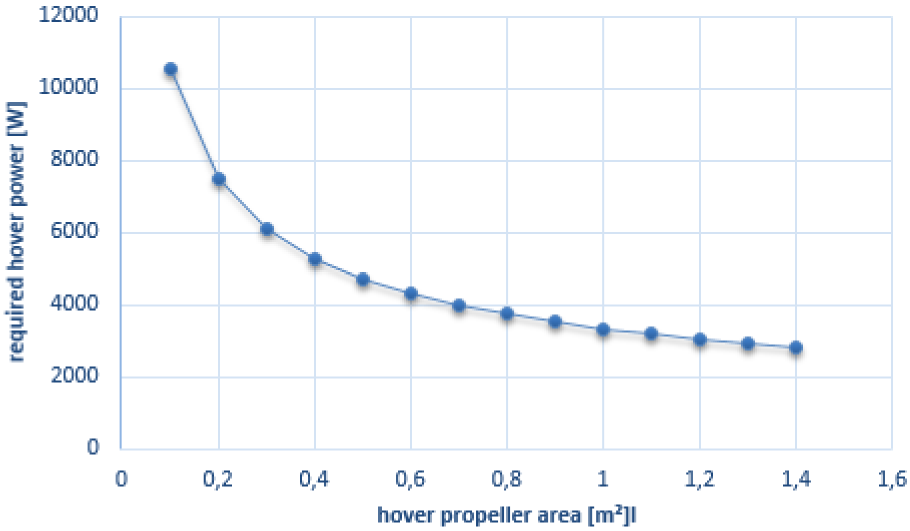

As it can be seen in the figure above as soon as the hover propeller area is bigger than 0,8m² the required power decreases only slowly. However, the bigger the propeller for the hovering the more drag is created by them during the conventional forward flight, which increases the power consumption during the conventional forward flight. In general, the size of the propeller disc is a result of an optimization process, which minimizes the mass of the overall propulsion system. The resulting disc size has an area of 0,8m², which leads to a propeller diameter of 0,7m for each of the two main lifting propellers. Using the formula in the figure below, one can estimate the required power for the engines. With an propeller efficiency of 85% the density of 1,22, the required power for each engine of the main lift propellers is then 2kW with a thrust to weight ratio of 1,1. This thrust to weight ratio has been chosen to have enough power for climb and roll control, which are both performed by the main lifting propellers.

iberall konstant ist, also der Luftstrom im Strahl sich wie ein Festkörper bewegt [2.6]. Nach dem Schub aufgelöst erhält man die sog. Bendemann'sche Formel $T = \sqrt[3]{2\rho A P^2}$ von 1910 [2.7], die den unter den genannten Verein-achungen ideell erreichbaren Schub bei gegebener Leistung berechnet.

6. Required power for secondary lift propellers and yaw control

The main task of these additional hover propellers is to compensate any disturbance force which is created by the horizontal stabilizer and the vertical tail. Moreover the control around the pitch axis and the yaw axis is performed with the help of these propellers. The needed thrust for the secondary lift propellers has been calculated in the following way. The maximum airspeed which should be compensated has been set to 10m/s. The maximum drag coefficient, which can appear is about 1,8 under 90° AoA/AoS. This leads to a maximum disturbance force from the horizontal stabilizer of about 28N. Consequently, the both secondary lift propellers have to compensate 28N and thus each of them has to be able to produce 14N thrust. With a propeller diameter of 250mm the needed power for each of the secondary lift motors has to be about 250W. Same has been performed with the yaw control and the needed power for these motors has been calculated to about 75W.

7. Landing gear

For the landing a 3point contact has been chosen since it is the minimum number of contacts needed to be statically determinate. The vertical tail exceeds downwards to provide the pusher propeller hitting on the ground and it serves as one of the contact points for the landing gears. The other two contact points are the end of the two rods extended from the fuselage. Their size is adjusted in a way that the main lift propellers' plane is parallel to the ground when landed, to prevent creating any side forces while landing. These two rods shall bend around the x-axis of the airplane to serve as a spring during landing. Moreover, the main portion of the total vehicle's weight is in the fuselage and during landing the biggest g-forces are expected. Thus, the mounting of the two rods is directly at the fuselage and consequently provides shortest force flow from ground to the main portion of the weight and reduces the load on the other parts of the aircraft. Another point is that the two front rods have a shape of a NACA airfoil to minimize drag and are as small as possible. In summary, the landing gear height is big enough to load the payload from the bottom of the aircraft without lifting or tilting the whole aircraft.

Landing gear for horizontal landing can easily be added for test purposes by installing wheels at the bottom of the three suspension points. In this design they are not mounted because the added weight and drag interfere with the initial goal of maximum aerodynamic efficiency.

8. Waterproofness concept and cooling

The aircraft is completely sealed. All four mounting surfaces (left wing to front fuselage, right wing to front fuselage, cargo bay to front fuselage, rear fuselage to front fuselage) are equipped with sealing rings and hence provide waterproofness of all mounting surfaces. The disadvantage of a complete sealed airplane is that the inner parts of the aircraft cannot be cooled with air from outside of the airplane. However, in the case of this aircraft the cooling of the inner components is performed with some heatpipes, which transport the heat to the fuselage surface and at the points where the heatpipes touch the fuselage's surface are additional copper plates to cool the heat pipe system via free airstream. The plates are installed on the lower back end of the fuselage directly under the main drive motor. The following figure shows the principle:

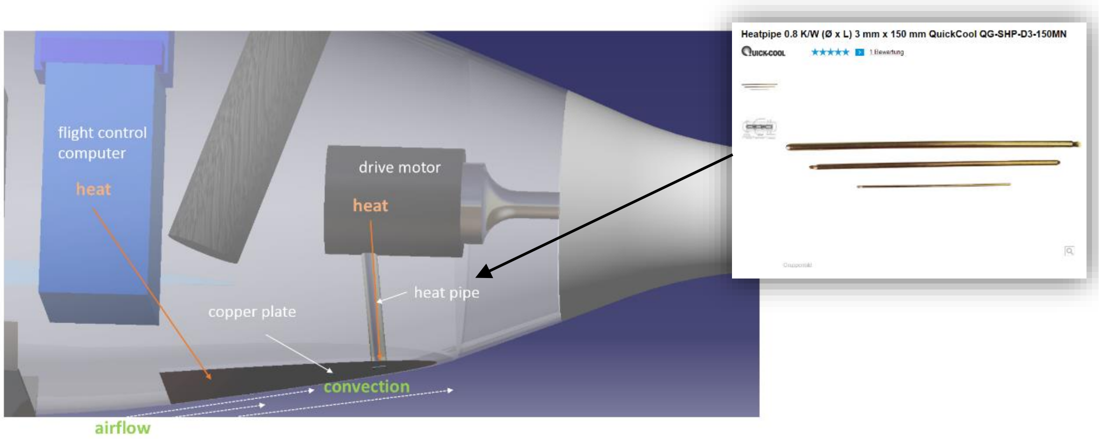

Because the battery is easily dismountable it can be stored in a climatized room with the ideal temperature. In case the temperature drops so much that the Li-Ion batteries could be damaged, a heating system will be activated. The battery management system uses circuits to balance the different cell voltages. These circuits and the included resistances can be used just like heating coils. In very cold conditions this will decrease the maximum travel distance to keep the batteries and the whole system safe. The battery cells chosen are Li-Ion 18655 cells (see systems sheet), which are already used in the tesla cars. This has the advantage that they are tested in all weather conditions under customer use and misuse. Thus, they are cheap and well known from an engineering point of view. Moreover, these cells are much more robust than coffee-bag cells as they already provide a stiff housing. Another point, which has driven the decision for Li-Ion cells than Li-Po cells is that they have a wider temperature range in which the can be operated and a wide operational temperature range is required.

9. Modularity / Ship-Ability

The aircraft consists of 5 modules:

- front fuselage
- the rear fuselage
- the left wing
- the right wing
- and the cargo bay module

None of these modules exceeds the maximum dimension of 2meters and has a single weight above 10kg, which makes it easy to carry each module by one person. The assembling is easy and fast as quick lock devices have been used and with the help of dowels the modules' mounting position is clearly defined and they have been used to transfer the forces and moments from one module to the other. Moreover, each mounting surface is equipped with a sealing ring to provide waterproofness.

10. Ease of Handling

The aircraft will be equipped with a fully autonomous autopilot, which is able to perform the cargo transport fully automatically. The aircraft can be loaded and unloaded with cargo and batteries in one step. The cargo module holds the payload and the battery pack, which can be easily changed in size for different shipping weights and travel distances. It can also be replaced by a sensor unit. The different modules are retained by quick locks and are accessible from the bottom as required. In case there is no automatic loading department beneath the aircraft, the modules can be changed from the front. This allows a user to unload the cargo safely because there are no propellers at the front side and therefor no striking danger when approaching the drone from this side.

When the cargo module is not mounted on the aircraft all other components like the Flight Control Computer or the main drive motor are easily reachable for maintenance or software updates.

11. Weight

Of course the main goal was not to exceed the maximum weight of 25kg. Furthermore it was critical for the aerodynamic design of the aircraft to have the overall center of gravity at the designed center of gravity point (45mm,0,0) to achieve the calculated aerodynamic behavior. It was possible to put all required parts for the propulsion and the ignition kit in the fuselage, so that the margin between the two points in x-direction was under 40mm.

Center of Gravity [mm]

Part	x	y	z	weight [kg]
FCC	-310	0	0	0,58
IMA	-145	0	-105	0,0575
ADS-B Transp.	-310	55	-94	0,155
Antennas	220	0	-100	0,322
FTP	0	0	-185	1,02
FTL	-420	0	-55	0,18055
Camera	467	0	10	0,483
COM	-309	0	-134	0,575
ADS	-310	-55	-106	0,127
Payload	30	0	10	5
Battery	330	0	0	7
Drive Motor	-500	0	0	0,38
Drive Motor Controller	-450	0	0	0,125
Drive propeller	-2317	0	0	0,08
Lift motor controller	100	0	-190	0,25
Lift motor & propeller	50	0	-190	0,86
Other motors & propellers	-1500	0	-50	0,324
Servos	-1300	0	50	0,4
Front fuselage	-95	0	-48	2,05
Rear fuselage	-1050	0	-2,6	1,52
Wings	420	0	-157	2,68
Payload Bay	76	0	118	0,72
	10	**0**	**-37**	**24,89**
Reference point	0	0	0	
Margin	**10**	**0**	**-37**	

12. Xfoil calculations

The Xfoil calculations have been used to estimate and design the aircraft aerodynamic qualities. For this purpose the main wing was calculated first. The mean aerodynamic chord and the wing span have already been set in the previous sections. The shape of the main wing has been adjusted in a way to achieve an almost elliptical lift distribution over the wing span. Therefore, small winglets have been added to the end of the wings. These winglets have moreover the task to provide the main lifting propellers striking the ground or any obstacles. Then the main wing has been tilted downwards to get a CM=0 at AoA=0°. The calculations for the main wing can be seen in the following figure:

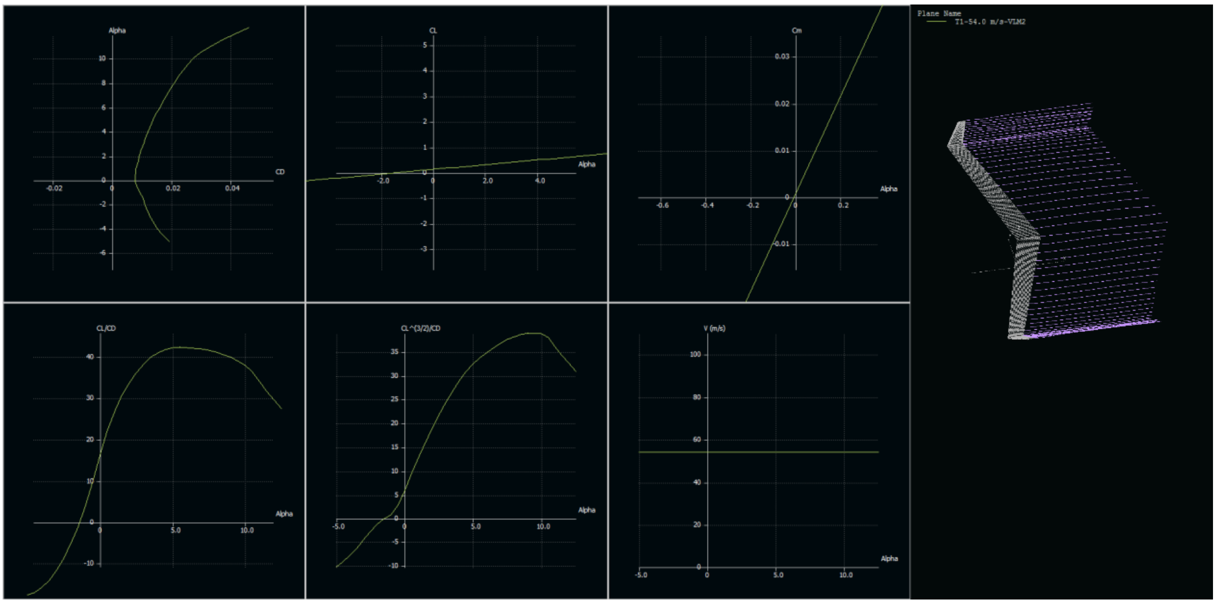

As it can be seen in the figure above, the wing achieves a maximum aerodynamic efficiency of 43 and the minimum drag coefficient is 0,0078 at AoA=0°. Moreover, the pitch moment derivative is zero at AoA=0°, which means that at 54m/s the aircraft can fly without load at the horizontal stabilizer. Then the horizontal stabilizer, the vertical tail and the fuselage have been added to the main wing and the results of the calculations can be seen in the following figure:

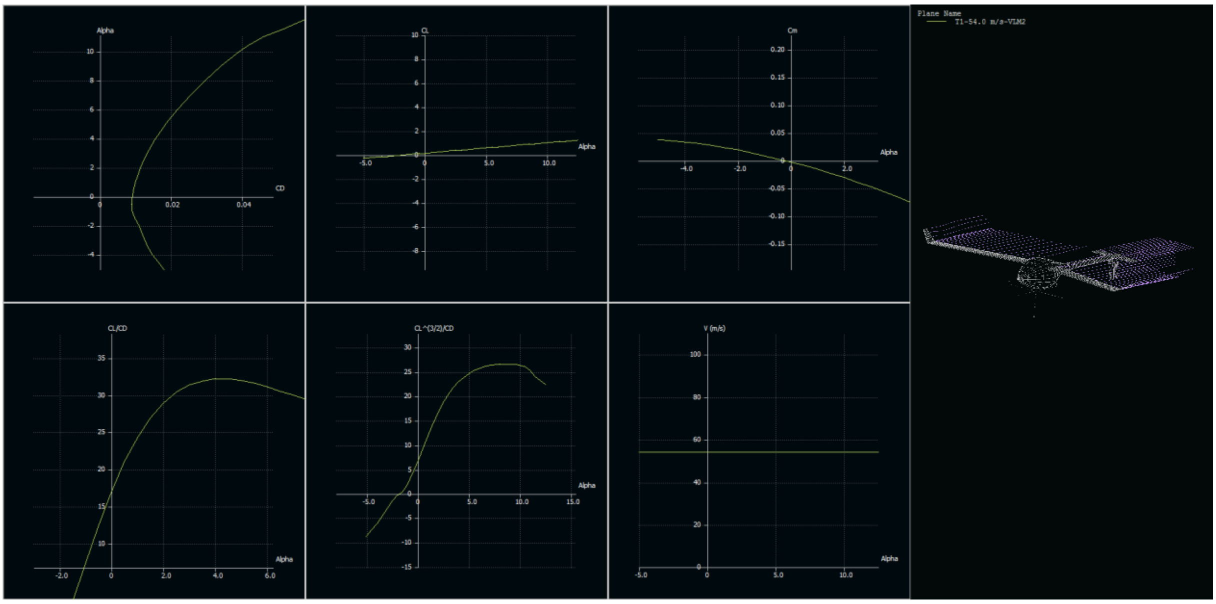

The whole aircraft has been designed to have about 10% static stability and as it can be seen in the figure above the pitch moment derivative has a negative slope, which corresponds to longitudinal stability. Moreover, the aircraft is trimmed at AoA=0° with the corresponding minimum drag value of 0,009. The Oswald efficiency factor has been estimated from the Xfoil calculations to 0,61 for the whole aircraft.

13. CD0 estimation

The resulting CD0 of the Xflr5 calculation is 0,009. However, Xflr5 does not take the fuselage into account. Hence the fuselage's drag has to be added first. The estimation of the fuselage's drag coefficient is based on the following formulas:

$$C_{D_{0_f}} = C_f f_{LD} f_M \frac{S_{wet_f}}{S}$$

$$C_f = \frac{0.455}{[\log_{10}(\mathrm{Re})]^{2.58}}$$

$$C_f = \frac{1.327}{\sqrt{\mathrm{Re}}}$$

$$\mathrm{Re} = \frac{\rho V L}{\mu}$$

$$f_{LD} = 1 + \frac{60}{(L/D)^3} + 0.0025\left(\frac{L}{D}\right)$$

$$f_M = 1 - 0.08M^{1.45}$$

The resulting CD0 of the fuselage is then 0,046. Moreover the skin friction drag of the hover propellers has been estimated to 0,013 and their pressure drag to 0,025. With additional drag for landing gear, pitot tube etc of 0,01, the total CD0 can be calculated to 0,0184.

14. Safety

In case the Flight Control Computer detects a failure in a critical component like one of the main lift motors, the battery pack shuts down and the parachute is deployed by the Skycat Launcher located on the main fuselage in backwards direction to help the parachute catch air. As already mentioned, all loading and charging activities performed by the user of the drone are done from the front side, while all propellers are on the other side of the main wing. In normal use there is no danger of touching any turning parts. Winglets slightly bent upwards and backwards restrict the access to the propellers even more.